Proceedings of Japan-France Seminar
J. Phys. Soc. Jpn. **65** (1996) Suppl. B pp. 181-187

Thermopower of $GdAl_2$ with Seesaw Heating System

K. YAGASAKI, T. NAKAMA, M. HIGA, E. SAKAI, A. T. BURKOV[1], E. GRATZ[2] and R. RESEL[3]

Department of Physics, University of the Ryukyus, Okinawa 903-01, Japan
[1]*A.F. Ioffe Physico - Technical Institute, Russian Academy of Science, St.Petersburg 184021, Russia*
[2]*Institute for Experimental Physics, Technical University Vienna, Vienna, Austria*
[3]*Institute for Experimental Physics, Technical University Graz, Graz, Austria*

An equipment for Thermopower (TP) measurements using DC-method in magnetic fields up to 17 T in the temperature range from 3 K to 300 K was constructed. A special heating technique named "Seesaw Heating" was developed and resulted in good thermal stability, better accuracy and a faster procedure. Chromel-Constantan thermocouples were utilized for measuring probes because of small and simple temperature dependence of magnetic field effect. Finding an empirical formula for all the calibration curves of TP of chromel enable us to measure TP at any field and at any temperature. The experimental results on $GdAl_2$ have been successfully analyzed on the basis of Mott's 2-band model with polarized conduction bands using linearized Boltzmann equation.

KEYWORDS: thermopower, reversal of the driving force, seesaw heating, $GdAl_2$, band splitting model

§1. Introduction

Generally, in order to cancel or reduce spurious voltages and to get accurate experimental data in DC measurements of transport properties, a conventional technique of driving field reversal has been commonly used; for example, current reversal for the electrical resistivity measurements, and current and magnetic field reversals for the Hall effect. However, such a conventional mechanical technique in measurement of the TP is not so common[1)] except for the AC technique. We introduce a special DC heating technique named "Seesaw Heating" , characterized by a fixed value of the heating power alternating between both ends of the sample, by which we can reverse temperature gradient of the sample without changing the sample temperature.[2)] It looks like AC method[3-5)] but, we believe, more than better than it. The Seesaw Heating method stands on measurements in the thermally steady state. We can measure the sign of TP and we can change widely the accommodation time and the heating power according with heat capacity of sample and environment and thermal coupling between them which change strongly with temperature.

It is very important to find the best thermocouples with the smallest magnetic effect and the simplest temperature dependence. We adapted chromel-constantan thermocouples [6,7)] for the sensor as the best material to the best of our knowledge.

Two calibration procedures, one of the relative thermopower of the thermocouple (Chromel - Constantan) and the other of the absolute thermopower of the reference material (Chromel), allow measurements in any magnetic fields up to 17 Tesla and at any temperature between 3 K to room temperature [8)].

We measured the TP of rare earth intermetallic compound $GdAl_2$ in magnetic fields of zero and 15 T. And the result was successfully analyzed on the basis of the molecular field model and Mott's 2-band model.

§2. The System

The principle of the Seesaw Heating is suggested in the upper part

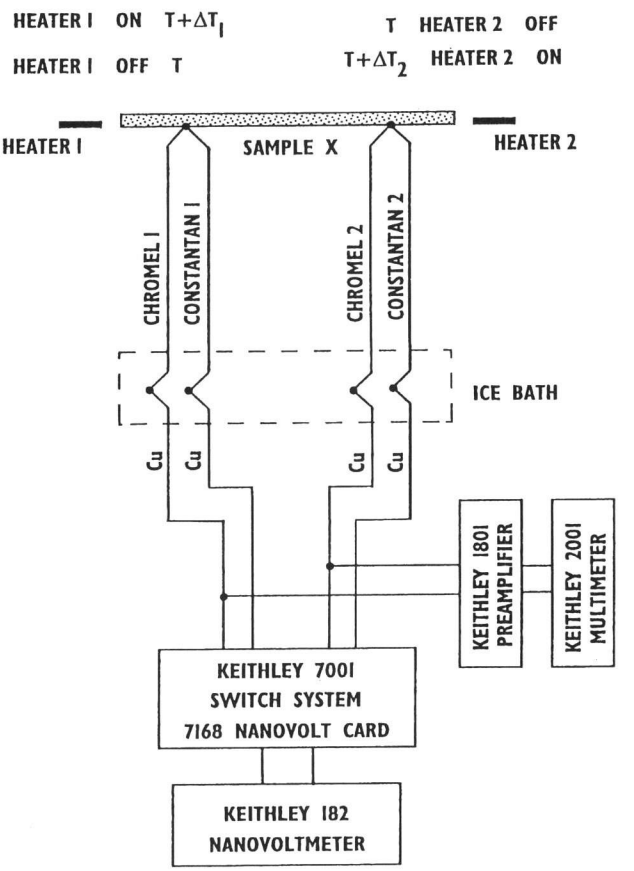

Fig. 1. Schematic sketch of the measurement circuits along the Chromel - Constantan thermocouples and Cu leads, also the equipment for the voltage measurements are indicated. The function of the Seesaw Heating is suggested above; the location of the heater is drawn symbolically besides the sample X.

of Fig. 1. Two heaters (denoted as heater 1 and heater 2) are drawn symbolically on either end of the sample X. The heaters work at a fixed heating power, they generate a temperature difference ΔT along the sample. During the time of the measurement always one of the two heaters is turningly switched on.

A characteristic time, the accommodation time, is necessary to change from the state $T + \Delta T_1$ and T (Heater 1 on) to the other state T and $T + \Delta T_2$ (Heater 2 on). Seesaw Heating allows to cancel spurious voltages of the measurement circuits. Due to the Seesaw Heating equal amounts of heat are supplied to the sample at any heater configuration, so the sample is not exposed to big temperature changes, which is better than the other methods where the gradient heater is working only at intervals.

The schematic illustration of the measurement circuits is also given in Fig. 1. Two Chromel - Constantan thermocouples are used as measurement leads. The switch system is configured to connect the four different leads to the input of a voltage measurement equipment. The output leads of the Chromel wires are connected directly to a second voltmeter.

Figure 2 shows the time dependent voltage, $V_{Chx}(t)$, of the Chromel measurement circuit (Chromel 1 - sample X - Chromel 2) and $V_{Cox}(t)$ of the Constantan measurement circuit (Constantan 1 - sample X - Constantan 2), for pure Pb used as the sample. Here, an accommodation time of 88 s was chosen. In the actual measurement, we take smaller accommodation times to reduce the influence of the time dependence in the spurious voltage. The chain saw-like voltage reaction of the measurement circuits is a result of the Seesaw Heating. Figure 2 also shows $V^{(1)}_{Chx}$ and $V^{(2)}_{Chx}$, thermoelectric voltage, generated in the Chromel measurement circuit and the corresponding voltages for the Constantan measurement circuit ($V^{(1)}_{Cox}$, $V^{(2)}_{Cox}$), the average of which measures the magnitude of spurious voltages. The extension expresses the temperature gradient along the sample ΔT_1 or ΔT_2, respectively.

Due to Seesaw Heating such a spurious voltage is canceled out to a few orders smaller than the original error as: 1) Small differences in the temperatures of the cold junctions of the thermocouple wires. 2) Offset voltage of a voltage measuring unit and noise pick up. 3) Chemical and mechanical inhomogeneity of the thermocouple wires.

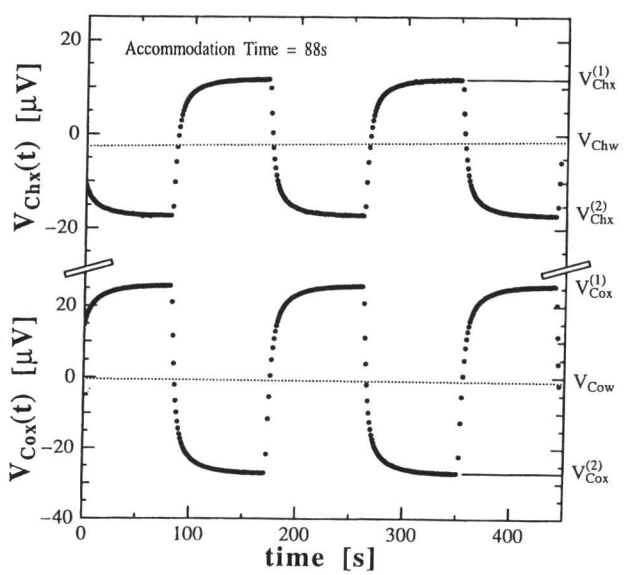

Fig. 2. Thermal e.m.f.s V_{Chx} and V_{Cox} as a function of the time t in response to Seesaw Heating. The accommodation time was chosen as 88 s, the heating power at 40 mW at a temperature of 300 K. The meaning of V^1_{Chx}, V^2_{Chx}, V_{Chw} and V^1_{Cox}, V^2_{Cox}, V_{Cow} is mentioned in the text.

§3. Cryogenic Design

The inner part of the sample holder is constructed symmetrically to get $\Delta T_1 \approx \Delta T_2$, although it is not a necessary condition for the measurements. A sketch of the sample holder is given in Fig. 3. The sample X with a minimum length of 9 mm is fixed with a help of the glass epoxy plate to the sample holder. The sample is pressed against two AlN plates, each AlN plate is fixed to a thin layer of Cu by low temperature glue. On each side of the sample, a conventional strain gauge is glued to this Cu layer as a heater. The strain gauges have a nearly temperature independent electrical resistance (R=120 Ω), and give quick response to any changes of heating current due to their small heat capacity. The thermal contact between the heater and the sample via Cu and AlN[9, 10] is good.

The thermal isolation between the heater parts (sample, AlN-plates, Cu-layer and strain gauge) and the heat sink is made from a glass epoxy material. The temperature of the heat sink is measured by a thick-film resistor, Cernox (Lake Shore Cryogenics, Inc.) [11], located in the middle of the heat sink. Its thermoelectric voltage does not depend on magnetic fields up to 15 T in the temperature range from 4.2 K to 300 K within 1.2%.

The thickness of the glass epoxy material is an important factor on the thermal response of the system, for the heat conductance and the thermal relaxation. The accommodation time should be as small as possible to reduce the influence of the time drift of the spurious voltages, which is about 20 s at low temperatures and about 40 s at room temperature. Also the heating power is strongly temperature dependent; 1 mW at 3 K and 20 mW at room temperature to establish a temperature difference of approximately $\Delta T_1 \approx \Delta T_2 \approx 0.2$ K.

The junction of the thermocouple pair is located at the end of the Al_2O_3 parts and pressed by a springs formed of a Cu-Sn-P alloy to sample surface. The above described inner part of the sample holder is surrounded by a Cu tube vacuum-sealed with a indium wire gasket. The temperature of the Cu tube is adjusted by a temperature controller using a second thick-film resistor mounted on the bottom of the Cu tube. At all temperatures, the cooling power is brought to the Cu tube mainly by a constant helium flow.

A configuration of the temperature gradient parallel to the magnetic field was set up to reduce the influence of other thermomagnetic effects like Ettinghausen - Nernst or Righi - Leduc effect.

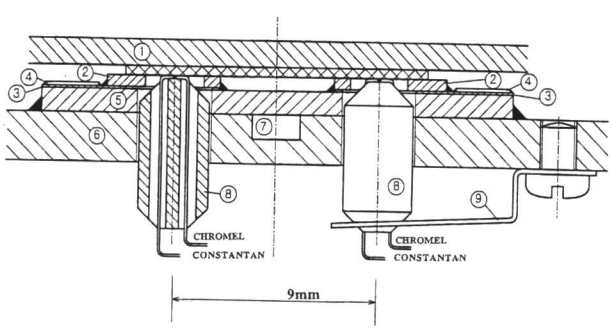

Fig. 3. Detail drawing of the inner part of the sample holder. The construction is symmetrical to the middle line. The sample is crosshatched; further notation of the parts: 1. glass epoxy material, 2. AlN plates, 3. Cu layers, 4. heater, 5. glass epoxy material, 6. heat sink, 7. temperature sensor, 8. Al_2O_3 parts, 9. spring.

§4. Calibration

For TP of the sample, we obtain

$$S_x(T,B) = S_{ch}(T,B) - \frac{V_{ch}S_{ChCo(T,B)}}{V_{Ch} - V_{Co}}. \quad (1)$$

V_{Co} and V_{Ch} can be obtained directly from voltage measurements, while the absolute thermopower of Chromel $S_{Ch}(T,B)$ and the relative thermopower between Chromel and Constantan $S_{ChCo}(T,B)$ must be determined as function of temperature and magnetic field by calibration.

The calibration of the thermocouples was done by two different experiments, one for the relative thermopower $S_{ChCo}(T,B)$, and one for the absolute thermopower $S_{Ch}(T,B)$.

The determination of S_{ChCo} was done by the usual integral method for each thermocouple. At zero field both thermocouples show the same temperature dependence of the thermal e.m.f.s which are in a good agreement with the literature values [12] (the observed deviations were smaller than 0.5%). The relative thermopower S_{ChCo} of the thermocouple reveals very small magnetic field dependence. In fact the effect of magnetic field of 15 T at 4.2 K was of order of our experimental resolution (0.1 μV/K). It implies that $\Delta S_{ChCo}/S_{ChCo} \leq 5\%$ which agrees with the standard data [6]. Because of this very weak magnetic field dependence of the relative thermopower we do not take this effect into account in the present work.

The absolute thermopower of chromel S_{ch} was reported to exhibit small magnetic field dependence [13-15]. At zero magnetic field at all temperatures we calibrated our reference electrode (chromel wire), using pure Pb (purity 99.999%) as the standard sample based on the table given by reports.[16] As the reference for the calibration of the chromel wires in the magnetic field we used two different materials:

1) Pure Pb was employed as the reference above 60 K[16]. It is known from literature [17] that above about 30 K TP of lead does not depend on magnetic field.

2) At lower temperatures we utilized superconducting $YBa_2Cu_3O_7$ compound (SC) with the superconducting transition temperature of 91 K in zero magnetic field, which is known to preserve the superconducting state below 60 K and in magnetic field below 17 T available from our magnet.

Figure 4 depicts the magnetothermopower (MTP) of chromel $\Delta S_{ch}(T,B)$, $(\Delta S_{ch}(T,B) = S_{ch}(T,B) - S_{ch}(T,0))$, as a function of temperature at 3, 6, 9, 12 and 15 T. $\Delta S_{ch}(T,B)$ is quite small, the biggest influence of magnetic field ΔS_{ch} is found around 50 K. ΔS_{ch} tends to zero at higher temperatures in good agreement with literature data. [14] The continuity between the low temperature SC-calibration and the high temperature Pb-calibration at about 60 K agree very well. The interpolation formula $f(T,B)$ is found empirically as follows:

$$f(T,B) = aTe^{bT^2} + cT^2e^{dT} \quad (2)$$

At first we got a function of field dependence of $S(T,B)$ at every 5 K below 100 K and at every 10 K above 100 K. Then we obtain all the coefficients of the eq. 2 as a function of field, using the $S(T,B)$ at all temperatures. Finally we succeeded to express all the data at every temperatures and in every magnetic fields by a single equation, eq. 2, within accuracy of 0.1 μV/K. The function gives s smooth interpolation of ΔS between the experimental points at all temperatures and magnetic fields as it is shown in Fig. 4. The results enable us to make accurate measurements of TP at any fields up to 17 Tesla and at any temperature between 3 K and 300 K. All the coefficients of the function $f(T,B)$ are listed in Table I.

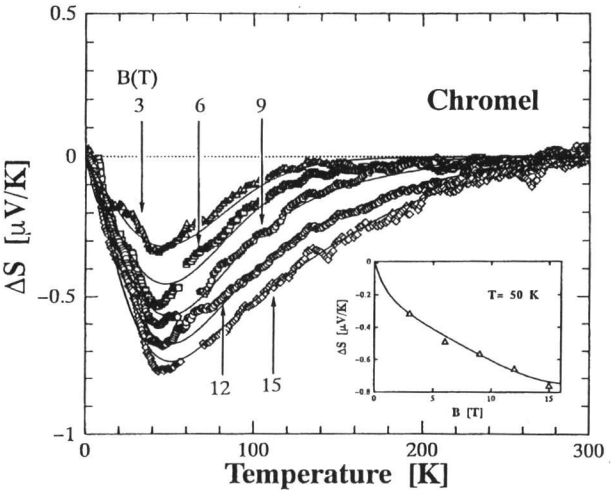

Fig. 4. The magnetothermopower (MTP) $\Delta S_{ch}(T,B) = S_{ch}(T,B) - S_{ch}(T,0)$ of the reference material Chromel obtained by calibration measurements (points) and the fitted correction function $f(T,B)$.

The great advantage of chromel wire reference is the comparatively small field dependence, especially at low temperatures where large effects are expected for other materials.

The accuracy of the measurement was checked by pure In. The literature values at zero Tesla are quite different [18,19], which may be due to different grain size or small content of impurities. We obtained an intermediate values in our measurement.

The variation of the TP with magnetic field is in good agreement with the literature [19]. The accuracy of the measurement in all temperature range is estimated to be at least within ± 1 μV/K, the relative accuracy within ± 0.1 μV/K.

§5. Thermopower of $GdAl_2$

Temperature dependence of the TP of $GdAl_2$ in zero and 15 T is shown in Fig. 5, together with the results obtained by Gratz et al.[20] and Sakurai et al..[21] It takes a large positive maximum around 20 K and it shows steep decrease from around 100 K to T_c=168 K. Its sign changes at a little below T_c to negative value and the value is almost constant above T_c. The experimental discrepancy at the paramagnetic region between our data and the previous ones is almost 1 μV/K. As we express below, we estimate the Fermi level of this sample is situated at the sharp peak of the density of the state above T_c. In such a case, very small shift of the Fermi level makes a very large change of the TP value. This experimental discrepancy could be dependent of the sample purity or chemical homogeneity. As we mentioned, the experimental error of our equipment is up to 1 μV/K in the largest estimation, the experimental discrepancy looks like just in the boarder value. The discrepancy below about 100 K is much larger than our experimental error limit, however the values are consistent within our experiments between measurements at zero field and 15 T. More detailed discussions should wait until we obtain the related sample properties such as the magnetization, electrical resistivity, magnetoresistance and high temperature TP. We will report these results and make a full discussion in near future. Here, aim of this paper is only to compare the difference between the results of measurements at zero field and 15 T and propose a model for the temperature dependence of the TP of $GdAl_2$ around the magnetic phase transition from the ferromagnetic to the paramagnetic.

The TP in the magnetic field of 15 T is a little smaller than that in

Table I. Empirical formula for the correction function $f(T, B)$ and the values of four fitting parameters a, b, c and d.

$$f(T,B) = aTe^{bT^2} + cT^2e^{dT}$$

$$a = \frac{2.10 \times 10^{-2} \times B}{-51.4 + 49.1 \times e^{-2.91 \times 10^{-2} \times B}}$$

$$b = -2.20 \times 10^{-4} - 1.02 \times 10^{-5} \times e^{0.187 \times B}$$

$$c = -4.18 \times 10^{-5} \times B$$

$$d = -7.47 \times 10^{-5} \times B^2 + 2.33 \times 10^{-3} \times B - 4.38 \times 10^{-2}$$

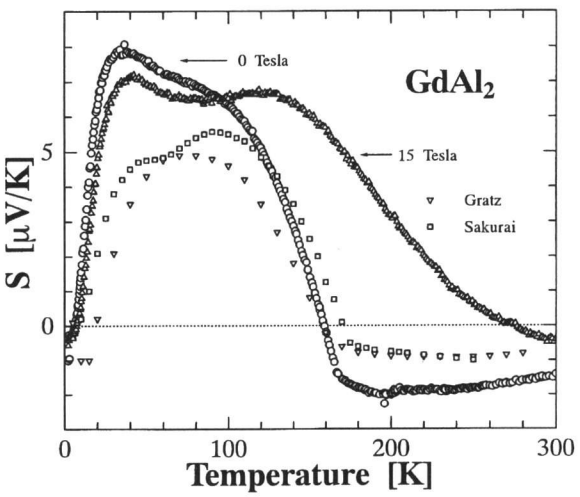

Fig. 5. Thermopower of $GdAl_2$ as a function of temperature at H = 0 and 15 Tesla, together with the results obtained by Gratz et al. and Sakurai et al..

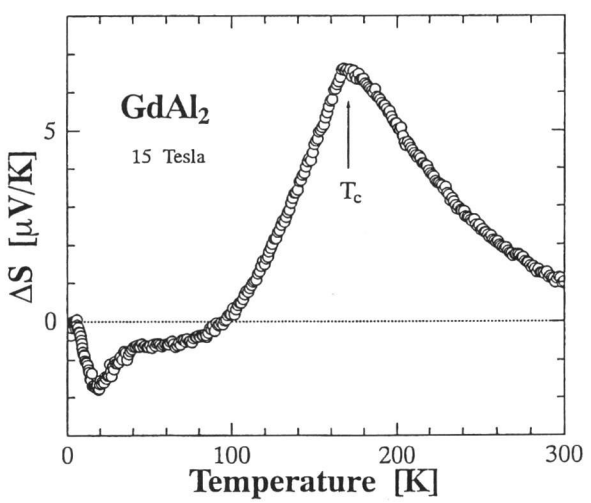

Fig. 6. Temperature dependence of magnetothermopower (MTP) $(S(H = 15\ T) - S(H = 0))$ of $GdAl_2$.

zero field below about 100 K, however, it is larger above the temperature and a big difference appears around T_c. The difference between them, the magnetothermopower (MTP), is shown in Fig. 6. It takes a large maximum at T_c and it also takes a small negative minimum around 15 K. This large MTP around T_c suggests that the sudden change of the TP at T_c is related with internal magnetic field acting on the conduction electrons.

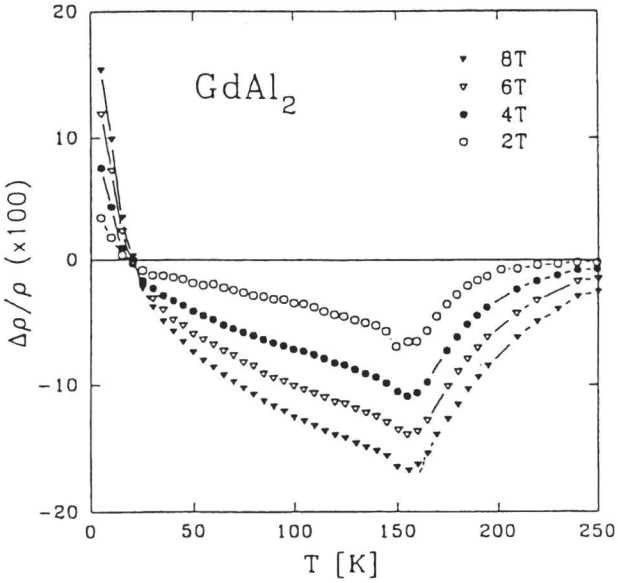

Fig. 7. Transverse magnetoresistance of $GdAl_2$ measured by Gratz et al..

Thus, this MTP measurement gives us the way to understand the temperature dependence of the TP of $GdAl_2$. Generally, we have two factors in how to model the transport properties, one is the electronic configurations and the other is the scattering mechanism. In the former factor, we have the single band model, the two-band model and so on, and also we treat the anisotropy (k dependence conductivity on the Fermi surface) and the energy dependence of the conductivity (related with DOS). In the latter factor, we have some scattering sources such as the electron-electron collision, phonon, magnetic moment, impurity, and so on. The MTP gives us important information about the transport mechanism for the each two factors. It suggests field effects on this ferromagnetic sample are very important and we need to take the effects for the two factors into account. We pick up here the field effects for DOS and for the magnetic moment arrangement. We will see them below.

This temperature dependence looks like the curve of the magnetoresistance of $GdAl_2$ obtained by Gratz et al.[22] as shown in Fig. 7. At first we will confirm these field induced properties, the MTP and the magnetoresistance, is due to induced magnetic moment by field, then, we propose a model for the TP of this compounds.

At a first step, we approximate the temperature dependence of the magnetization by the Brillouin function with S=7/2 for Gd as follows;

$$I = \frac{N \sum_{S_z=-S}^{S} (-2\mu_B S_z) \exp\left(\frac{-2\mu_B S_Z(\omega I + H)}{k_B T}\right)}{\sum_{S_z=-S}^{S} \exp\left(\frac{-2\mu_B S_Z(\omega I + H)}{k_B T}\right)}$$
$$= 2N\mu_B SB(2\mu_B S(\omega I + H)/k_B T)$$
$$= 2N\mu_B SB(\alpha), \qquad (3)$$

where I is magnetization, ω, molecular field constant, H, applied field, and $B(\alpha)$, Brillouin function.

Figure 8 shows the calculated magnetization in magnetic fields H = 0 and 15 T, and also Fig. 9 is temperature dependence of the induced magnetization by the field of H=15 T. The induced magnetization has a sharp peak at T_c. The magnetic resistivity is given by the mean square fluctuation of the localized spin and is expressed assuming the RKKY interaction as follows[23],

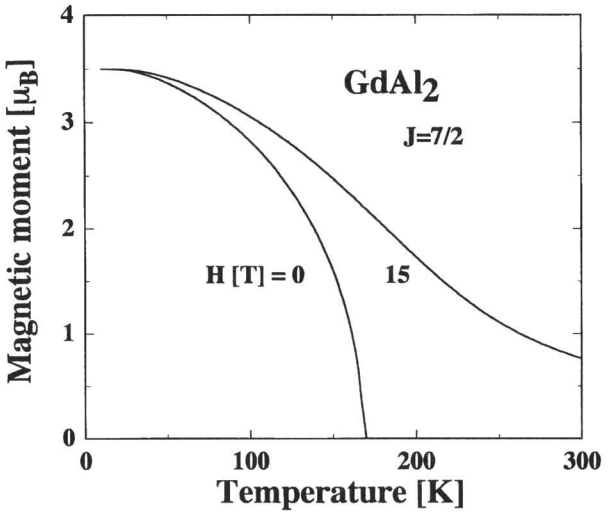

Fig. 8. Temperature dependence of $4f$ magnetization in fields of zero and 15 T according to Brillouin function.

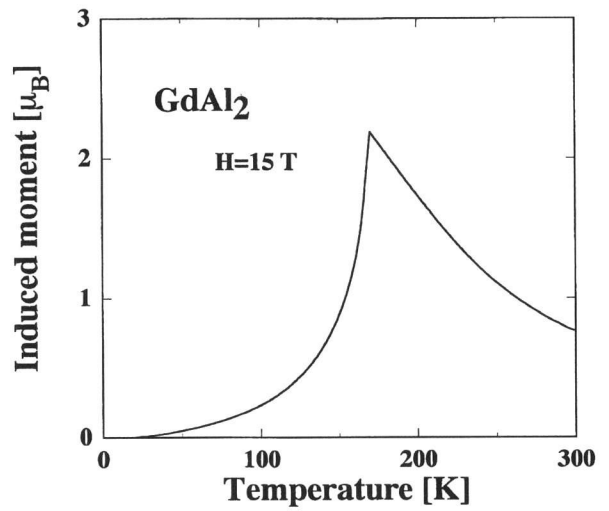

Fig. 9. Temperature dependence of calculated induced magnetic moment by the field of 15 T .

$$\rho_{mag} \propto (S-\nu)(S+\nu+1). \tag{4}$$

where S and ν are $4f$ spin and averaged spin at a temperature, respectively. It should be noted that eq. 4 expresses only the scattering mechanism assuming no change of the electron configuration. After calculation of the magnetoresistance at H=15 T according to eq. 4, we find a clear minimum at T_c and it could explain the experimental magnetoresistance as a first approximation. These theoretical rough confirmation of temperature dependence suggest that the MTP can be given by the induced magnetization and the TP itself is related deeply with the magnetization. However we have no change of MTP and almost no temperature dependence of TP if we assume the Fermi surface is spherical and DOS does not change, because TP is the ratio of the energy transfer to the momentum transfer and the energy transfer is given by the conduction difference between above and below the Fermi surface, which depend on DOS. Temperature dependence of TP of the ferromagnetic metal was calculated by Ausloos and Durczewski[24] by calculating TP tensor of anisotropic ferromagnetic metals with localized magnetic moments based on the Boltzmann equation . In their calculation, the Fermi level and density of states (DOS) are supposed to be fixed and to correspond to free electrons and they treat the anisotropic scattering matrix assuming Mott's formula for the TP. Here in this paper, we will calculate the TP in complete different way from their assumption. We pay no attention on the detailed feature on the Fermi surface and treat it by free electron model (Mott's 2-band model). The essential point of our model is taking into account the energy dependent conductivity over (above and below) the Fermi surface in detail. We don't use the Mott's formula (the expression by energy derivative of conductivity on the Fermi surface) which is assumed energy dependent conductivity is linear over the Fermi level, but we use the original formula of the TP because the Fermi level move across the sharp peak of DOS in our approximation, in that case the energy dependent conductivity cannot be approximated by linear function (see below).

The TP appears only when the energy dependent conductivity (spectral conductivity) varies asymmetrically over the Fermi level, and the spectral conductivity is related with DOS in metal. Therefore, TP varies largely when the asymmetry of DOS changes around Fermi level. It is not always effected directly by the temperature dependence of conductivity. For example, some metals do not show any change of the TP at the crystallographic transition temperature even if the resistivity changes largely.[25]

In our calculation, the energy dependence of DOS cannot be treated as linear because the Fermi level gets across a sharp peak and DOS curve is not linear within k_BT; TP should be expressed by the original linearized Boltzmann equation as follows:

$$S(T) = -\frac{1}{eT}\frac{\int_0^\infty \sigma(\epsilon,T)\left(-\frac{\partial f^0}{\partial \epsilon}\right)(\epsilon-\mu)d\epsilon}{\int_0^\infty \sigma(\epsilon,T)\left(-\frac{\partial f^0}{\partial \epsilon}\right)d\epsilon}. \tag{5}$$

We also assume the internal field acting on the conduction electrons due to the external field and RKKY molecular field does not depend on the energy position of the conduction electron near the Fermi level. This assumption gives a result that the spectral conductivity can be divided into energy dependent part and temperature dependent part clearly within the linearized approximation, as we focus only on the conductivity depending on magnetic moments. Here, the temperature dependent part is originated only by the scattering mechanism in the same meaning as eq. 4, and the energy dependent part is given by the DOS changing.

$$\sigma(\epsilon,T) = \sigma(\epsilon)\theta(T), \tag{6}$$

where, $\sigma(\epsilon)$ is energy dependent part of the conductivity, and $\theta(T)$ is its temperature dependent part. Generally, such a division could be accepted when the nature of the scattering mechanism and the electronic structure is not changed significantly. However if our assumption is applied, $\sigma(\epsilon)$ and $\theta(T)$ are completely independent each other and the division can be hold even if the electronic structure changes much. Thus, temperature dependent part of the conductivity of denominator and numerator cancels out with each other in the equation of S, and the TP is contributed only by the energy dependent conductivity or shape of DOS curve around the Fermi level. The obtained TP is expressed as follows:

$$S(T) = -\frac{1}{eT}\frac{\int_0^\infty \sigma(\epsilon)\left(-\frac{\partial f^0}{\partial \epsilon}\right)(\epsilon-\mu)d\epsilon}{\int_0^\infty \sigma(\epsilon)\left(-\frac{\partial f^0}{\partial \epsilon}\right)d\epsilon}. \tag{7}$$

On the other hand, the electrical conductivity is given as follows:

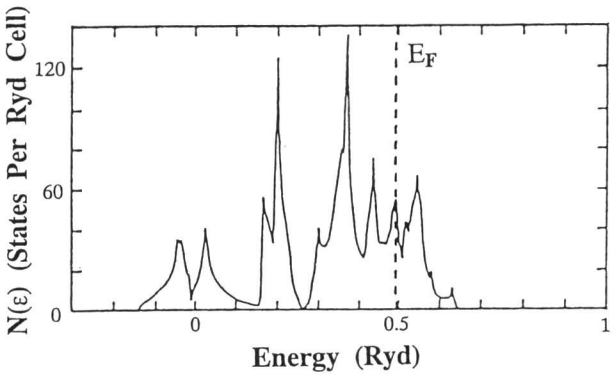

Fig. 10. DOS curve of $LaAl_2$ obtained by Hasegawa and Yanase.

$$\Sigma(T) = \frac{1}{\rho(T)} = \theta(T)\int_0^\infty \sigma(\epsilon)\left(-\frac{\partial f^0}{\partial \epsilon}\right)d\epsilon. \tag{8}$$

If the integral part of the above description in eq. 8 is constant in the whole temperature range, we get eq. 4 as $\theta(T)$ for magnetic resistivity.

According to Hasegawa and Yanase,[26] Fermi surface of $LaAl_2$ is composed of 7th and 8th band's hole sheets and 9th band's electron sphere, and the Fermi level is situated at the top of sharp peak of DOS as depicted in Fig. 10, which is mostly d-character. Burkov et al.[27] explained measured results of the resistivity and TP of $La_xY_{1-x}Al_2$ alloy by linearized Boltzmann equation assuming Mott's free electron 2-bands model.[28,29]

It can be reasonably assumed that the Fermi surface of $GdAl_2$ is similar to that of $LaAl_2$. We focus on the sharp peak just around the Fermi level in Fig. 10 and approximate the DOS around the Fermi level by a model composed of a peak overlapped by a wide flat band. The DOS of the peak is approximated by Lorentzian and denoted d band and the wide flat band is denoted as s band.

We adopt the same model, Mott's 2-band model, for the band configuration around the Fermi level of $LaAl_2$ as Burkov et al. In the Mott's 2-band model, the conduction is carried mainly by s band electrons. The DOS of s band, $N_s(\epsilon)$, is constant over a very wide range of energy and therefore s band itself gives no contribution to the TP, even if it carries the electrical conduction mainly. The conductivity of the d electrons is roughly one order smaller than that of the s electrons but DOS of d band, $N_d(\epsilon)$, is pretty larger than that of s band. The scattering probability is proportional to the Fermi surface area, and thus the relaxation time of the s band is proportional mainly to inverse of the d band's DOS due to $s-d$ scattering. As a result, the TP is proportional to inverse of the d band's DOS: the effective conductivity for the TP is given by the Mott's 2-band model as follows:

$$\sigma(\epsilon) \propto \frac{1}{N_d(\epsilon)}.$$

Due to the RKKY interaction, the conduction electron feels the molecular field which is proportional to the averaged $4f$ spin, and the bands split. The Zeeman splitting of the conduction electron is proportional to the total field composed of molecular and applied field. Thus it is reasonable to explain the temperature dependence of the TP is due to changing of the Fermi surface caused by the polarization (Zeeman splitting) of the conduction band around T_c and in the magnetic field.

The best fitted Lorentzian for the DOS is asymmetrical in which half width of the higher energy side is a little larger than the lower side.

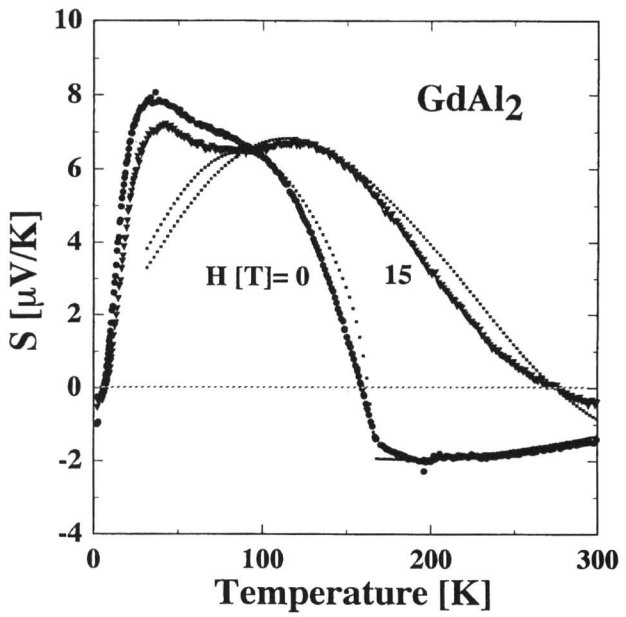

Fig. 11. The calculated results for Thermopower at $H = 0$ and 15 T together with the experimental results of $GdAl_2$.

$$N_d(\epsilon) = \frac{1}{2}\frac{\beta^2}{(\epsilon-b)^2+\beta^2} + \frac{1}{2}\frac{\beta^2}{(\epsilon+b)^2+\beta^2}, \tag{9}$$

where, $2b$ is band splitting width proportional to the molecular field and the external field, and the numerical value of β in k_B units is as follows;

$$\beta = \begin{cases} 485 & \text{(for the left half of each Lorentzian curve)} \\ 515 & \text{(for the right half of each Lorentzian curve)} \end{cases}$$

The number of the conduction electrons are conserved under the band shift:

$$n = \int_0^\infty (N_d(\epsilon) + N_s(\epsilon))f^0(\epsilon, T)d\epsilon = constant. \tag{10}$$

We also obtained a height of the flat s band DOS about a third of the height of d band DOS as a best fit to the experimental data. Here, it should be noted that the electrical resistivity is not so affected by the d band splitting because we assume s band conductivity is very large and its energy dependent conductivity does not change around the Fermi level.

Figure 11 shows the calculated results together with the experimental results. The theoretical curves at H=0 and 15 T agree essentially with the experimental ones around T_c. At the paramagnetic temperature region, the Fermi level is situated a little right side from the top of the DOS peak, and shifts to the left side of the down spin band peak in the ferromagnetic temperature. Owing to this shift, S is a little negative value in the paramagnetic region and passing through zero when the Fermi level is just at the top, then increases with decreasing temperature. On the other hand, at low temperature region the coincidence of the calculated value to the experimental one is poor, where we need some additional data and information for more discussion.

The aim of this paper is to demonstrate the band splitting model is effective for the TP around the ferromagnetic transition in $GdAl_2$. We can successfully understand the mechanism of the temperature dependence of TP by Mott's 2-band model. However, the other band model such as the usual single or 2-band models *etc.* could also be applicable

to the band structure of $GdAl_2$. We need to see which is the best model for this system.

According to this model, we have two channels of transport properties caused by the magnetic moments: one is the direct scattering process and the other is changing of DOS by the internal field. The electrical resistivity depends mainly on the former one and the TP mainly on the latter. Varieties of the temperature dependence of the TP could be presented by the position of the Fermi level in DOS and the shape of DOS. We will discuss the transport properties of the other rare earth ferromagnets in future.

1) P.M.Chaikin and J.F.Kwak: Rev. Sci. Instrum. **46** (1975) 218.
2) R. Resel, E. Gratz, T. Nakama, M. Higa, K. Yagasaki and A. T. Burkov; Review of Scientific Instruments **67(1996)1970**.
3) R. H. Freeman, J. Bass: Rev. Sci. Instrum. **41** (1970) 1171.
4) D. Korn, W. Murer: Z. Phys. B **27** (1977) 309.
5) W. H. Kettler, R. Wernhardt, M. Rosenberg: Rev. Sci. Instrum. **57** (1986) 3053.
6) A. von Middendorff: Cryogenics 11 (1971) 318.
7) H. H. Sample, L. J. Neuringer, L. G. Rubin: Rev. Sci. Instrum. **45** (1974) 64.
8) D. B. Richards, L. R. Edwards, S. Legvold: J. Appl. Phys. **40** (1969) 3836.
9) R. B. Dinwiddie, A. J. Whittaker, D. G. Onn: Int. J. Thermophys. **10** (1989) 1075.
10) AlN plates received from Tokin Corporation, Sendai, Japan.
11) Performance specification for model-CX1050. Lake Shore Cryogenics, Inc.
12) International Reference Tables acc. to IEC 584-1 Degussa Germany (1977) .
13) K. Schroder, M. Otooni: J. Phys. D: Appl.Phys. **4** (1971) 1612.
14) C. K. Chiang: Rev. Sci. Instrum. **45** (1974) 985.
15) G. S. Abilov, B. I. Alshin, V. M. Beilin, L. A. Medvedeva, N. G. Flerov: Instrum. Exp. Tech. **26** (1983) 239.
16) R. B. Roberts: Phil. Mag. **36** (1977) 91.
17) A.D. Caplin, C.K. Chiang, P.A. Schroeder: Phil. Mag. **30** (1974) 1177.
18) B. Bosacchi, R. P. Huebener: J.Phys.F:Met.Phys. **1** (1971) L27.
19) A. D. Caplin, C. K. Chiang, J. Tracy, P. A. Schroeder: phys.stat.sol. (a) **26** (1974) 497.
20) E. Gratz and M. J. Zuckermann: J. Magn. Magn. Mater. **29** (1982) 181.
21) T. Yamamoto, J. Sakurai and Y. Komura: J. Phys. Collq. C5 **40** (1979) 120.
22) E. Gratz: unpublished (1992), J. L. Fournier and E. Gratz: Handbook on the Physics and Chemistry of Rare Earth, Vol.**17**, edited by K.A.Gschneidner, Jr., L.Eyling, G.H.Lander and G.R.Choppin, North-Holland, Amsterdam (1993) 409.
23) T. Kasuya: Prog. Theor. Phys. **15** (1956) 58.
24) M. Ausloos and K. Durczewski: J. Magn. Magn. Mater. **53** (1985) 243.
25) M. Kurisu, H. Kadomatsu, H. Fujiwara, T. Ohyama, J. Sakurai and Y. Komura: J. Phys. Soc. Jpn. **56** (1987) 3240.
26) A. Hasegawa and A. Yanase: J. Phys. F Metal Phys. **10(5)** (1980) 847.
27) A.T.Burkov, M.Vedernikov and E.Gratz: Physica B **176** (1992) 263.
28) N. F. Mott: Proc. Phys. Soc. **47** (1935) 571.
29) N. F. Mott: Proc. Roy. Soc. A **147** (1935) 396.